

# TIME-DEPENDENT PHASE-SPACE MAPPING OF SPACE-CHARGE-DOMINATED BEAMS\*

D. Stratakis#, Brookhaven National Laboratory, Upton, NY 11973

R. A. Kishek, R. B. Fiorito, I. Haber, M. Reiser, J. C. T. Thangaraj, and P. G. O'Shea, Institute for Research in Electronics and Applied Physics, University of Maryland, College Park, MD 20742

K. Tian, Thomas Jefferson National Accelerator Facility, Newport News, VA 23606

## Abstract

In this paper we report on a proof of principle experiment for demonstrating the possibility of reconstructing the time resolved-phase-space distribution by tomography which provides us with far more information than a time-sliced emittance. We emphasize that this work describes and demonstrates a new methodology which can be applicable to any beam pulse using imaging methods with the appropriate time resolution for the pulse duration. The combination of a high precision tomographic diagnostic with fast imaging screens and a gated camera are used to produce phase space maps of two beams: one with a parabolic current profile and another with a short perturbation atop a rectangular pulse. The correlations between longitudinal and transverse phase spaces are apparent and their impact on the dynamics is discussed.

## INTRODUCTION

A high brightness and low emittance beam is *a priori* requirement for X-ray Free Electron Lasers, higher-luminosity high-energy colliders, and Spallation Neutron Sources. However, the longitudinal charge distributions rarely take the form assumed in theory and instead almost always contain structure. Such complicated pulse shapes have been shown to result in space-charge wave production, beam expansion and longitudinal energy spread [1]. Thus, knowledge of the time-sliced parameters of the beam such as current, energy spread, emittance and phase space orientation is an important requirement to understand their evolution.

Recent experiments [2, 3] using time dependent imaging techniques showed, in fact, that the transverse beam distribution is affected by longitudinal perturbations. However, these previous studies measured the beam only in configuration space, and any knowledge of phase-space was inferred either from simulations or were applied to beams with low to mild space-charge forces [4].

In this study, by combining our tomography diagnostic with fast-imaging techniques, we report on a proof of principle experiment for demonstrating the possibility to reconstruct the time-resolved phase space by tomography which provides as with far more information than at time-sliced emittance. The method includes a linear correction to account for the space-charge. We report high resolution phase-space maps within a 3 ns and 10 ns gated window

of two beams: one with a parabolic current profile and another with a short perturbation atop a rectangular pulse.

## PHASE-SPACE TOMOGRAPHY

Tomography is related to a theorem by Radon who stated that an object in  $n$ -dimensional space can be recovered from a sufficient number of projections onto  $(n-1)$  dimensional space. In the area of beams tomographic techniques can recover the phase space distribution of a beam from a large number of projections of the phase space onto configuration space. The projections are images of the beam obtained by rotating the phase space through a given angle by altering the strength of a focusing magnetic field upstream of the imaging screen [3,5,6]. Tomographic techniques typically involve quadrupoles to rotate the phase space distribution but recent improvements, developed tomography to use solenoids [6] also. The reconstruction algorithm incorporated the effects of linear space charge forces. In our present experiment, following the discussion described in Ref. 6 we apply such solenoidal tomography to recover our transverse beam phase-spaces. We note that to verify the technique, we simulated it using 200 particle-in-cell code simulations to generate the projections, and compared the phase-space obtained directly from simulation to that reconstructed from the data. For the purpose of the discussion here suffice it to say that the agreement is surprisingly good given all the assumptions.

## EXPERIMENTAL DETAILS

Our present experiment was carried out on the Long Solenoid Experiment (LSE) [3] (Fig. 1). Our transport line consists of a thermionic electron gun, two short solenoids, S1, and S2 and a phosphor screen located immediately downstream of the solenoids (we call this location: LC1). The electron gun is a variable-perveance gridded gun and the beam energy was 5 keV. The solenoids are located 13.1 cm and 29.5 cm from the aperture and a Bergoz fast current transformer between them is used to measure the beam current. As described in Ref. 6, for our tomographic reconstruction we varied the magnetic field strengths of the two solenoids incrementally 48 times and obtained a beam image for each setting at a phosphor screen location 43 cm downstream.

The screens to image the beam consist of a ZnO:Ga phosphor deposited on a quartz plate produced by Lexel Imaging Systems, Inc.. The phosphor emits in the near UV with peak close to 390 nm and the decay time is 2.4

\*Work supported by U.S. Department of Energy High Energy Physics and Fusion Energy Science.

#dikty@bnl.gov

ns. Then, a variable gate, intensified charged-coupled device camera PIMAX2 was used to capture the beam distributions generated on the screen in 3 or 10 ns gate sample times within the 100 ns beam pulse.

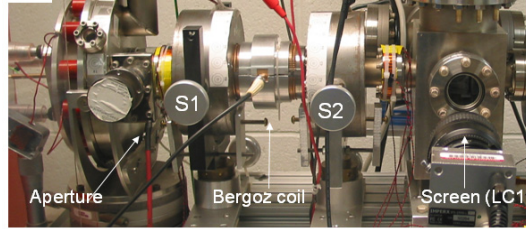


Figure 1: LSE experimental configuration.

To investigate the evolution of longitudinal perturbations we intentionally produced density modulations close to the beam source by modifying the electronics of our gridded electron gun. In this type of the gun, a grid is able to gate the output beam by being biased negatively relevant to the cathode to impede current flow. A beam is born when a positive pulse is applied to the grid making it positive with respect of the cathode, thus allowing electrons to be emitted. The pulse is generated by a cathode pulse system and is transported through a transmission line. The longitudinal perturbation is created by connecting a cable at the middle of the pulse generation transmission line through a “T” connector. Small changes in the bias voltage produce large changes in the output current. Furthermore, by manipulating the pulse generation circuit of the electron gun with a low pass filter we can create beams with parabolic beam shapes. More details about the generation of perturbations can be found in Ref. 2.

### RECTANGULAR PULSE WITH PERTURBATION

For our experiment the bias voltage was set at 55 V leading to a negative perturbation. The current profiles, measured at the Bergoz coil, with and without perturbation are illustrated in Fig. 2(a). The measured beam current without perturbation was 25 mA and the width of the perturbation was about 7 ns and it corresponds to about 80% of the total beam current. A 10 ns gate is applied to the ICCD camera to obtain time-resolved images of the charge particle beam on the screen. The gate is applied along the negative perturbation part of the beam. Then, the phase space was reconstructed and then, the same experiment is repeated but with the perturbation turned off.

Figure 3 shows the beam distributions at LC1. The first row indicates the beam image on the screen and the second shows the corresponding tomographic reconstructed phase spaces at that location when the perturbation is off (left column) and when its on (right column). Clearly, the distributions look very different: First, in configuration space the beam sizes are not equal and the beam with perturbation looks smaller, possibly due to the different focusing it experiences relevant to the main beam. Interestingly, the measured emittance from

the reconstructed phase-spaces when the perturbation is on ( $37.0 \pm 4 \mu\text{m}$ ), is higher relevant to the case when it is turned off ( $28.0 \pm 3 \mu\text{m}$ ). We believe that this is due the higher space-charge intensity that the beam has when the perturbation is on as showed in recent experiments [2]. Note that the emittance growth between the aperture and LC1 appear to be larger when the perturbation is on relevant to the case when the perturbation is off.

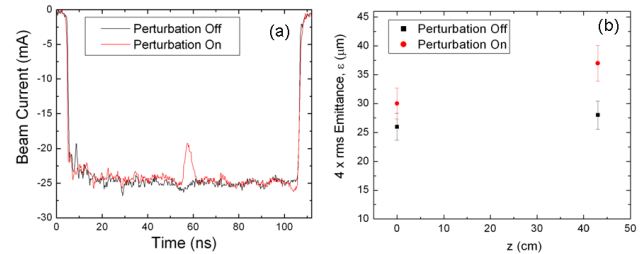


Figure 2: (a) Beam longitudinal current profile with and without perturbation; (b) Measured by tomography emittances ( $4 \times rms$ ) at  $z=0$  and  $z=43$  cm.

The larger emittance growth could be due the transverse mismatch caused by the initial higher space-charge [2] of this beam at  $z=0$ cm. A second reason could be the effect of the gate window (10 ns) integration over smaller time slices. During this time period the perturbation is varying rapidly, so what we measure could be also integrated smear of many phase spaces resulting in a larger emittance. Future experiments with a smaller gate width are underway and will address this issue in more detail elsewhere.

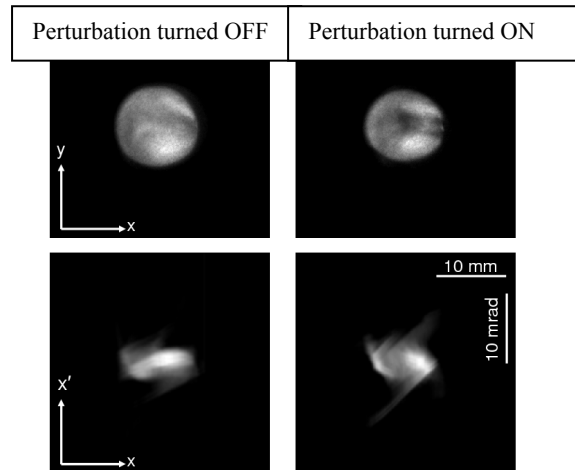


Figure 3: Beam distribution in configuration space (top row) and phase-space (bottom row).

To compare the time-sliced tomography results to ordinary, integrated, tomography we repeated the experiment described above but this time we increased the gate width to 100 ns so as to encompass the entire beam pulse. Details can be found in Ref. 3. The major conclusion was that we couldn't distinguish between the two cases (perturbation off and perturbation on); either in configuration space or in phase-space. To quantify any differences, we calculated the beam emittances and found that they differ by less than 1%. Hence, in contrast to

time-resolved measurements, time integrated measurements did not reveal any significant differences in the transverse beam distribution when a beam was propagating with and without longitudinal perturbation.

## PARABOLIC BEAM PULSE

We now turn to the parabolic beam. For the experiment, the measured peak current of our 60 Hz, 5 keV beam was 23.5 mA, the pulse length was 60 ns and the bias voltage was set at 60 V. Figure 4 shows the longitudinal current profile from the signal at the Bergoz FCT, as well as the position of the slices used in our phase-space measurement.

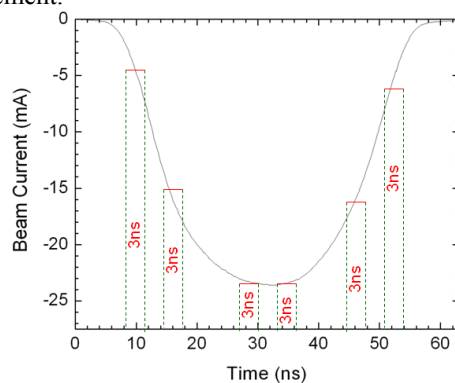


Figure 4: Parabolic beam pulse.

By setting the ICCD camera gate window at 3 ns, and moving it progressively from the beam head toward the tail we can collect a number of beam images at the screen (LC1), each corresponding to a 3-ns beam slice. Figure 5 (top) shows the resulting beam distribution in configuration space for the six different slices. Examination of Fig. 5 indicates that the slices vary in size.

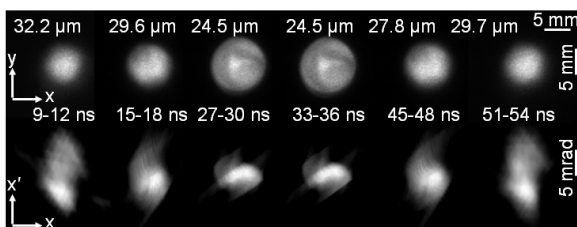


Figure 5: Time-resolved beam images (top) and phase spaces (bottom) for the parabolic beam shown in Fig. 4. Measurements are done at LC1.

Figure 5 also shows the measured phase space by tomography in LC1. Both configuration space images and the phase space distributions reveal a detailed structure that differs from slice to slice. Part of the structure inside the phase space arises from the non-uniform distribution at the gun cathode. As pointed in Ref. 6 such structure scales with the beam intensity. Therefore, since its each slice of the parabolic bunch has a different current, the space charge forces experienced by each slice differ, and henceforth the final structure of the phase-space differs as well.

Furthermore, like the configuration space images, the phase spaces depend on the position along the beam; both exhibit symmetry about the peak of the pulse. The inset in Fig. 5 (first line) shows the measured beam  $4 \times rms$  slice emittance at LC1 from the time-resolved phase-spaces. Note that given that the tomography measured error is about 10%, our results do not reveal any significant emittance difference between the aperture and LC1. However, the emittances are higher at the edges with respect to the center at both locations. Note especially the rapid variation of the beam current within the edge slices Fig. 4. Then, as in the case of the perturbed rectangular beam, the phase space orientation can change within the image integration gate, resulting in an apparent enlargement of the distribution in phase space. Furthermore, the tomography analysis assumes a constant, “average”, current within each slice, which is clearly not the case in the ends. One solution for this problem would be to decrease the camera gate window so that the variation in current within each slice is reduced.

## CONCLUSIONS

In summary, in this paper we reported on a proof of principle experiment for demonstrating the possibility of reconstructing the time resolved-phase-space distribution by tomography. It should be noted that this tomography diagnostic is not restricted to fluorescent screens. Hence, an interesting thought is the possibility to generalize the tomography technique described in this paper to high energy (5-100 MeV range), short pulse (sub ps range) electron beams such as needed in the injectors for short-pulse X-ray FELs, for example, the Linac Coherent Light Source [7]. It may be possible to apply slice tomography to images collected by Optical Transition Radiation (OTR) [8], which has a sub-ps response, in combination with a faster gated ICCD or using streak camera, if the beam is reproducible from shot to shot.

## REFERENCES

- [1] M. Reiser, Theory and Design of Charged Particle Beams (John Wiley & Sons, Inc. New York, 1994).
- [2] K. Tian *et al.*, Phys. Plasmas. **15**, 056707 (2008)
- [3] D. Stratakis, R.A.Kishek *et al.*, Phys. Rev. ST. Accel. Beam. **12**, 020101 (2009)
- [4] D. H. Dowell *et al.*, Nucl. Instrum. Methods Phys. Res., Sect. A **507**, 327 (2003); I. Ben-Zvi *et al.*, Proceedings 1997 PAC Conference p. 1971.
- [5] D. Stratakis, R.A. Kishek *et al.*, Phys. Rev. ST. Accel. Beam. **9**, 112801 (2006)
- [6] D. Stratakis, *et al.*, Phys. Plasmas **14**, 120703 (2007)
- [7] R. Akre *et al.*, Phys. Rev. ST. Accel. Beam. **11**, 030703 (2008)
- [8] R. B. Fiorito *et al.*, these proceedings.